Z. Phys. C – Particles and Fields 48, 525–541 (1990)

Zeitschrift für Physik C Particles and Fields

Search for collective transverse flow using particle transverse momentum spectra in relativistic heavy-ion collisions*

Kang Seog Lee[1], U. Heinz[2], E. Schnedermann[2]

[1] Department of Physics, Chonnam National University, Kwangju 500, South Korea
[2] Institut für Theoretische Physik, Universität Regensburg, Postfach 397, D-8400 Regensburg, Federal Republic of Germany

Received 28 February 1990; in revised form 4 June 1990

Abstract. The particle transverse momentum spectra recently measured in relativistic heavy-ion collisions at CERN and BNL are analysed within an expanding fireball model. All the particle spectra at a given beam energy can be reproduced simultaneously with a single set of intensive parameters for the initial state of the fireball. As typical freeze-out parameters in this beam energy region we find a freeze-out temperature $T_f \simeq 110$ MeV for most hadrons, and an average transverse expansion velocity at freeze-out of $\langle v/c \rangle \simeq 0.4 - 0.45$. The striking enhancement at transverse momenta $p_T < 200$ MeV/c in the CERN pion data cannot be fully explained by the existence of transverse flow.

1 Introduction

Nuclear collisions at relativistic energies are expected to form hot and dense nuclear matter under extreme conditions. According to QCD, a phase transition to a deconfined phase of quarks and gluons may occur under such circumstances. A prerequisite for the formation of a quark–gluon plasma is the deposition of a large amount of energy in a small collision region. Therefore, in order to assess the chances for creating a QGP in present or future relativistic heavy-ion collision experiments, it is necessary to establish the collision dynamics and to prove the formation of a hot and dense initial "fireball" from the recent experiments at the CERN SPS and the Brookhaven AGS.

In this paper we analyse the measured hadronic particle spectra from those experiments and argue that they provide evidence for the formation of the fireball and its subsequent collective expansion.

This work extends and improves upon a previous analysis [1] in which we successfully fit the pion transverse momentum spectra with an expanding fireball model, i.e. by a superposition of local thermal motion and global collective expansion. In this model we start from an initial state specified by the initial energy density and the initial baryon density, $(\varepsilon_0, \rho_{b,0})$, and then we follow the expanding system along an isentropic path in the phase diagram until freeze-out. For each particle species the freeze-out temperature is estimated via a kinetic freeze-out criterion which compares the scattering time scale and expansion time scale. Assuming at the freeze-out point local thermal equilibrium momentum distributions in each fireball volume element, superimposed by a global collective expansion, the particle spectra can be obtained by Lorentz-transforming a local Boltzmann distribution with the collective expansion velocity profile into the laboratory frame. By varying the initial state of the fireball, an excellent fit to the pion momentum spectra measured by the WA80 [2] and NA35 [3] collaborations in central 200 A GeV O + Au collisions was obtained [1]. We noted that the generally concave shape of the pion transverse momentum spectra (which in a parametrization in terms of purely thermal emission requires the introduction of two or more sources with different temperatures) is nicely reproduced by including the additional flow component, except perhaps an unexplained excess of negative pions in the NA35 data (also seen by NA34 [4, 5]) at very low transverse momenta ($p_T < 200$ MeV/c). Hard scattering contributions which lead to a flattening of the pion spectra above $p_T \sim 1.5 - 2$ GeV/c in proton–proton and proton–nucleus collisions [6], and for which indications are also seen in peripheral nucleus–nucleus collisions [2], appear to be completely covered by the collective flow component in central nucleus-nucleus collisions up to $p_T = 2.8$ GeV/c [1, 2].

We pointed out, however, that a fit to the pion spectra alone is not sufficient evidence for the validity of the underlying picture, and that a conclusive separation of thermal and flow components in the spectra requires a simultaneous study of the p_T-spectra of heavier hadrons. The reason is that the influence of a collective flow *velocity* on the observed hadron *momentum* increases with the mass of the hadron, while (at a given temperature) the average *thermal momentum* is the same

* Work supported in part by Deutsche Forschungsgemeinschaft (DFG), grant He1283/3-1, and by the Korean Science and Engineering Foundation (KOSEF), grant 893-0202-002-2

for all particle species. Spectra for more massive particles have recently become available from the same CERN experiments mentioned above [7–9] and will therefore be studied in this paper as a test for our flow hypothesis. We will find that the same set of initial fireball parameters used for the pion spectra also yields a good fit to the proton and Λ transverse spectra, i.e. all spectra appear to show the same combination of random thermal motion and transversally directed collective flow.

Furthermore, the E802 collaboration at Brookhaven have recently measured [10, 11] transverse mass spectra of π^+, π^-, K^+, and K^- mesons, protons, and deuterons in central Si + Au collisions at 14.5 A GeV. These spectra will also be analysed with our model, and we will see that again a single set of fireball initial conditions, leading to a well-defined combination of thermal and collective motion at freeze-out, yields a good description of all these spectra. Models which do not incorporate a flow component must postulate strongly varying freeze-out temperatures for different particle species for which no theoretical motivation exists. We will take the success of our model at both BNL and CERN energies as direct evidence for collective flow in the directions transverse to the beam.

The situation with longitudinal flow is much less clear-cut: Experimentally [10] the slope parameters extracted from the BNL proton spectra vary with rapidity y as the inverse of cosh y. A qualitatively similar behaviour has now been confirmed for the pion slope parameter [11]. This agrees with a spherically symmetric, purely thermal distribution, while the y-variation predicted from our spherically expanding fireball model appears to be somewhat flatter. This failure of the model is expected, since it probably indicates a non-spherical component in the expansion flow. This will be studied in a future paper, employing an extension [12] of the model which uses only cylindrical symmetry. Different flow velocities in the longitudinal and transverse directions are even more evident at the higher CERN energies, where e.g. the measured rapidity distribution of produced charged particles [3, 13] is much wider than any spherical model predicts [13]. This points to a strong longitudinal flow component in the experiment, due to either partial transparency [14] in this case or to the strongly anisotropic expansion of an initially highly longitudinally compressed Fermi–Landau fireball [15].

The spectra of K^+ and K^- mesons are of special interest as they may contain information on the formation of a quark-gluon plasma [16]. We find, however, that the still insufficient statistics of the available kaon data does not yet allow for a clear conclusion on this point. The E802 collaboration also measured [11] a large K^+/π^+ ratio of $\sim 20\%$ in these collisions while the K^-/π^- ratio was lower, $\sim 4\%$. These numbers, as well as the observed strong increase [10] of these ratios with p_T, will also be studied here in the context of our model.

Throughout this paper we will work with transverse mass ($m_T = \sqrt{m^2 + p_T^2}$) rather than transverse momentum (p_T) spectra. As is well known [17], purely thermal radiation produces a transverse momentum spectrum

$$dN/p_T dp_T \sim (m_T/T) K_1(m_T/T) \sim \sqrt{m_T/T} \exp[-m_T/T]$$

which, if plotted logarithmically against m_T, looks nearly like a straight line, with a very slight convex modulation by the prefactor. Any deviations from such a behaviour, such as a concave curvature of the spectrum and different slopes for different particles, are then cleanly identifiable and indicate deviations from purely thermal behaviour with fixed temperature. If plotted against p_T instead, the same thermal spectra exhibit a shoulder in the region $p_T < m_0$ which forbids a clean interpretation of the (strongly varying) spectral slope in this region and, through its mass dependence, tends to obscure the interesting mass dependent effects from a possible collective flow which were mentioned above.

The paper is organized as follows: In Sects. 2 and 3 our model is explained with particular focus on recent improvements of our earlier version [1]. In Sect. 4, various particle spectra measured by the NA34, NA35 and WA80 groups at CERN and by the E802 collaboration at Brookhaven are analysed within our model. The p_T-dependence of the K^+/π^+ and K^-/π^- ratios is calculated and compared with the data. Our conclusions are presented in Sect. 5.

2 Model for the fireball evolution and freeze-out

As mentioned in the introduction, we will restrict our discussion entirely to spherically symmetric systems. Since the main focus of the paper is on transverse dynamics, and all longitudinal coordinates are integrated over, this restriction is not expected to be very crucial while it considerably simplifies the description. However, we will see the model fail as soon as rapidity (i.e. longitudinal momentum) dependencies are analyzed. A strong longitudinal flow at freeze-out appears to be necessary to explain the observed rather broad rapidity distributions, and it could considerably influence our estimate of the initial energy density if it were also caused by hydrodynamical effects (as in the Landau model) and not a remnant of the fireball initial conditions, due to partial transparency. A more general cylindrically symmetric analysis is under way [12].

Since a detailed explanation of our model was presented elsewhere [1], only its main features and a few recent improvements [12] will be described in this section. Three stages of the heavy-ion collision are considered. 1) The initial stage of the collision when a hot and dense fireball is formed and evolves towards local thermal and chemical equilibrium. Most of the entropy of the fireball is generated at this stage. 2) Expansion stage: The expansion will be adiabatic and maintain local thermal equilibrium. Chemical equilibrium is also assumed throughout this stage, but is not crucial for the shape of the particle spectra (although it would be for their absolute normalization, which we do not discuss). 3) Freeze-out stage: Thermal equilibrium breaks down at this stage and particles decouple from the collective expansion; they then stream freely into the detectors where they deliver information on the local temperature and collective flow velocity at freeze-out.

2.1 *Initial stage – formation of the fireball and its equation of state*

During the initial stage of a nucleus-nucleus collision, a fireball is formed which is described in terms of its initial energy density ε_0 and baryon density $\rho_{b,0}$. The entropy of the fireball is generated by converting part of the kinetic energy of the incident nuclei into random thermal motion in the fireball. We do not specify how this conversion of energy happens, and how it gets equilibrated; also we do not require full stopping, i.e. full conversion of the beam energy into thermal motion, although in this case the picture employed below of a *spherical* fireball would perhaps be best justified. The assumption of local equilibrium is a drastic approximation of our model and needs to be justified by a kinetic analysis which is beyond our present abilities. We consider it as a working hypothesis subject to experimental tests. The initial state parameters (ε_0, $\rho_{b,0}$) cannot be reliably calculated and thus are taken as fit parameters in our analysis of various hadron spectra. In a more microscopic description they would depend on the amount of stopping experienced by the nuclei, i.e. on the fraction of beam energy initially converted into internal excitation of the fireball. The values extracted from the data by this procedure can in the end be used to gain qualitative insight into the initial stopping and pre-equilibrium processes.

We do not assume vanishing baryon number in the collision zone, as is often done in the description of the central rapidity region at ultrarelativistic energies. Rather, we assume that, for a reasonably central heavy-ion reaction, the fireball contains all the baryons from the (so far) smaller projectile nucleus and a fraction of the target nucleons contained in the tube swept out by the impinging projectile. For central O + Au collisions this picture yields $A_{FB} = 16 + 52 = 68$, for central S + S we have $A_{FB} = 32 + 32 = 64$, and for central Si + Au collisions $A_{FB} = 28 + 75 = 103$.

Through an equation of state, which assumes a hadronic resonance gas in thermal and chemical equilibrium, all other thermodynamic quantities are expressed in terms of the temperature T, and the baryon and strangeness chemical potentials, μ_b and μ_s. The resonance gas contains all members of the baryon and meson ground state octets, the η' and ρ mesons, the Δ resonance, and all their antiparticles. The condition of vanishing net strangeness in the fireball throughout the evolution (implied by the absence of weak processes due to the short collision time) determines the strangeness chemical potential μ_s as a function of T and μ_b.

From the initial temperature and chemical potentials, also the initial specific entropy S/A can be determined which crucially influences the further evolution of the system.

2.2 *Expansion stage – isentropic expansion*

The hot and dense fireball expands hydrodynamically under its high internal pressure. We assume that in this stage the initially produced entropy is approximately conserved which can be justified (at the 10–20% level) by kinetic analyses [18, 19]. During isentropic expansion, the system cools and dilutes; the thermal energy per baryon decreases which means that part of the initial thermal energy has to convert into collective flow energy. This adiabatic conversion of thermal energy into expansion flow is governed by the hydrodynamic equations. Through their solution for a specific (say, stationary) initial condition we would obtain the collective velocity field $\boldsymbol{\beta}(r,t)$ for each fireball volume element as it developes in time. Since (in view of our poor control over the pre-equilibrium stage) the choice of initial conditions is to a large extent arbitrary and must in the end be justified by comparison with experiment, the hydrodynamically calculated flow profile at later times can only be as realistic as the chosen initial condition.

Therefore, we use an alternative and much more economical approach: we calculate from the condition of entropy conservation an expansion trajectory [20, 21] in the phase diagram, $\rho_b(T)$, and for each point of this trajectory we assume the form of the velocity profile $\boldsymbol{\beta}(r)$. Since in the end the hadronic spectra are only determined by one point of this trajectory, the freeze-out point T_f, we actually need the velocity profile only there, and parametrizing its shape at freeze-out is as good as fixing the initial flow conditions for a hydrodynamic calculation.

Given the shape of the velocity profile, which we can adjust by varying the power n in the following parametrization for spherical expansion:

$$\boldsymbol{\beta}(r,T) = \left(\frac{r}{R(T)}\right)^n \beta_s(T)\mathbf{e}_r, \tag{2.1}$$

the scales $\beta_s(T)$(= surface velocity) and $R(T)$(= radius of the expanding fireball) are determined by baryon number and energy conservation:

$$A = \int_\sigma j^\mu(r,T)d\sigma_\mu(r); \quad E_{TOT} = \int_\sigma T^{0\mu}(r,T)d\sigma_\mu(r). \tag{2.2}$$

Here $\sigma(r)$ is any (spherically symmetric) space-like hypersurface with cartesian components $\sigma_\mu(r) = (\sigma_0(r),\ r\sin\theta\cos\phi,\ r\sin\theta\sin\phi,\ r\cos\theta)$, for example a surface of constant local or of constant global time. Its normal vector

$$d\sigma_\mu = -\varepsilon_{\mu\nu\lambda\rho}\frac{\partial\sigma^\nu}{\partial r}\frac{\partial\sigma^\lambda}{\partial\theta}\frac{\partial\sigma^\rho}{\partial\phi}dr\,d\theta\,d\phi \tag{2.3}$$

(with $\varepsilon_{\mu\nu\lambda\rho} = -\varepsilon^{\mu\nu\lambda\rho}$ being totally antisymmetric and normalized by $\varepsilon^{0123} = +1$) takes the form

$$d\sigma_\mu = d^3r\left(1, -\frac{\partial\sigma^0}{\partial r}\mathbf{e}_r\right). \tag{2.4}$$

Inserting this and the ideal fluid decomposition $j^\mu = \rho_b u^\mu$, $T^{\mu\nu} = (\varepsilon + P)u^\mu u^\nu - Pg^{\mu\nu}$ with $u^\mu = \gamma(r)(1, \beta(r)\mathbf{e}_r)$ into the conservation laws (2.2), we obtain

$$A = 4\pi \int_{\sigma^0(r)} r^2 dr\,\gamma\,\rho_b\left(1 - \frac{\partial\sigma^0}{\partial r}\beta\right); \tag{2.5}$$

$$E_{TOT} = 4\pi \int_{\sigma^0(r)} r^2 dr\left[\gamma^2(\varepsilon + P)\left(1 - \frac{\partial\sigma^0}{\partial r}\beta\right) - P\right] \tag{2.6}$$

($\gamma = 1/\sqrt{1-\beta^2}$). The radial integrals have to be performed from 0 to the fireball radius R (which is not yet known, but to be determined by these equations) along the specified hypersurface, i.e. for each value of r the integrand has to be evaluated at the corresponding time resp. temperature. We will discuss two specific choices for this hypersurface in more detail below.

To avoid confusion it should be noted that the specific shape (2.1) of the expansion velocity profile is postulated *along the hypersurface* $\sigma^0(r)$; so the same parametrization for different hypersurfaces corresponds to different choices for the profile. Fortunately, we found the results to be not very sensitive to the detailed shape of the profile (e.g. the power n), as long as the general features (zero expansion velocity in the fireball center, maximum expansion on the surface) remain intact. For the two hypersurfaces discussed below, among the choices $n = 0.5$, 1, and 2 the value $n = 2$ always gave a slightly better fit to the experimental spectra than the other values (this agrees with our intuitive expectation that flow begins at the surface and only later proceeds inward, leading to a concave flow velocity profile), so we will from here on fix $n = 2$ in (2.1).

2.3 *Freeze-out*

As the fireball expands, its density decreases, resulting in ever longer mean free paths for the particles, Furthermore, due to the growing rate of collective expansion, all the particles recede from each other increasingly fast, thus further reducing the rate of particle–particle collisions. At some point, local equilibrium (the basis of hydrodynamics) can no longer be maintained and the particles freeze out, i.e. they decouple from the collective hydrodynamical flow and stream freely into the detectors.

These considerations show that freeze-out is a kinetic process and cannot be properly described in a hydrodynamical language. Cascade simulations of the hadronization and expansion process for a quark–gluon plasma [22] show that the points of last interactions for the emitted hadrons are widely scattered in space-time, i.e. they do not occur along a sharp and well-defined "freeze-out surface". However, by connecting the points of largest density in such a scatter plot, an idealized freeze-out hypersurface can be defined, although such a definition should in principle allow for fluctuations to simulate its intrinsic fuzzyness. In this paper we will not be able to account for this latter stochastic aspect, but we will try to incorporate the basic kinetic features of freeze-out by determining our idealized freeze-out hypersurface from kinetic arguments [16], rather than by just fixing it to occur at a certain critical temperature, energy density, or baryon density as is usually done [23, 24].

We will use as freeze-out criterion [25] that it should occur when the mean collision time begins to exceed the rarefaction time scale,

$$\tau_{\text{scatt}} > \tau_{\text{expansion}}, \tag{2.7}$$

i.e. when during the time it takes the particles to transverse one mean free path by their thermal motion, they have collectively receded from each other by the order of one more mean free paths. We have checked that in our applications this generally occurs before the mean free path exceeds the size of the fireball, and that thus the dynamics is more important for freeze-out than the finite nuclear size.

At each point T of the expansion trajectory, the scattering time scale is determined, for each particle species separately, by the expression

$$\tau^{(i)}_{\text{scatt}}(T) = \frac{1}{\sum_j \langle v_{ij}\sigma_{ij}\rangle_T \rho_j(T)}, \tag{2.8}$$

where the sum is over all particle species, $\langle v_{ij}\sigma_{ij}\rangle_T$ is the relative velocity between the scattering particles times their total cross section at the appropriate collision energy, averaged over a thermal distribution with the temperature T, and $\rho_j(T)$ are the partial densities of the particle species at the same temperature. We use an approximate form for this expression [1, 12] which, as far as the cross sections are concerned, treats all baryons as nucleons and all mesons as pions; also, instead of performing a proper thermal average, we take the thermal velocity of the lighter collision partner times a representative cross section from the particle data booklet in the momentum region corresponding to a thermal distribution with temperature T. Still, through the cross sections the formula is particle-specific, i.e. it predicts earlier freeze-out of weakly coupled particles (e.g. K^+ mesons in a baryon-rich environment [16]) than of strongly coupled particles (pions and nucleons).

The rarefaction time scale for a spherically expanding fireball with the velocity profile (2.1) is approximately given by [12]

$$\frac{1}{\tau_{\text{expansion}}(r,T)} \simeq (n+2)\frac{\beta(r,T)\gamma(r,T)}{r}. \tag{2.9}$$

Nonrelativistically ($\gamma \equiv 1$) this timescale is r-independent for a linear velocity profile ($n = 1$) such that in this case freeze-out occurs homologously (i.e. at the same time resp. temperature) across the entire fireball. Relativistically, and also for other velocity profiles, this is no longer true, and our freeze-out criterion predicts that different shells of the fireball freeze out at different temperatures. However, once one considers taking into account this effect, one should for consistency also include realistic temperature and density profiles from the beginning. This is presently being studied, for both spherical and cylindrical expansion geometries [12]. Here, however, we will neglect these complications and simply evaluate $\tau_{\text{expansion}}$ on the surface, postulating instantaneous (in either local or global coordinates, see below) freeze-out as soon as the freeze-out criterium is satisfied on the fireball surface. (Since we are here using homogeneous density distributions this simplification should not be too unreasonable.)

2.3.1 Freeze-out at constant local time. The transformation between global (i.e. fireball center-of-mass) coordinates (t, r) and local coordinates $(\bar{t}, \bar{r})$ attached to the fluid elements in the fireball is given by a radial Lorentz boost with the flow velocity $\beta(r)$ at the position of the

fluid element:

$$\gamma t - \gamma\beta r = \bar{t};$$
$$\gamma r - \gamma\beta t = \bar{r}. \tag{2.10}$$

A surface of constant local time is defined locally by $d\bar{t} = 0$, leading to the relation

$$\gamma dt - \gamma\beta dr = 0$$

between the differentials in the global frame. Thus the complete surface of constant local time $\bar{t}$ can be obtained by solving the differential equation

$$\frac{dt}{dr} = \beta(r, t), \tag{2.11}$$

if the velocity profile along this surface is known.

For this subsection we will assume that freeze-out is to occur across the entire fireball at constant local time once the freeze-out criterion (2.7) is satisfies at the surface. We model the fireball using constant temperature and baryon density profiles from 0 to R along space-time slices of constant local (or "proper") time, such that freeze-out occurs automatically at a constant temperature T_f. The radius R_f of the fireball at freeze-out and the amount of collective flow at this point (i.e. the value of β_s) are determined through energy and baryon number conservation, (2.5/6), which for a constant-local-time hypersurface with $\partial\sigma^0/\partial r = \beta$ (2.11) read [26]

$$A = 4\pi \int_0^{R_f} \gamma\rho_b(1-\beta^2)r^2 dr = \frac{4\pi}{3} R_f^3 \rho_{b,f} f_n(\beta_s), \tag{2.12}$$

$$E_{\mathrm{TOT}} = 4\pi \int_0^{R_f} \varepsilon r^2 dr = \frac{4\pi}{3}\varepsilon_f R_f^3, \tag{2.13}$$

where (with $\xi = r/R_f$)

$$f_n(\beta_s) = 3\int_0^1 \frac{\xi^2 d\xi}{\gamma(\xi)} = 3\int_0^1 \xi^2 \sqrt{1-\beta_s^2\xi^{2n}}\, d\xi. \tag{2.14}$$

From (2.13) and $E_{\mathrm{tot}} = (4\pi/3)\varepsilon_0 R_0^3$ we obtain immediately the freeze-out radius

$$R_f = R_0\left(\frac{\varepsilon_0}{\varepsilon_f}\right)^{1/3}, \tag{2.15}$$

while β_s is obtained from (2.12) by solving

$$f_n(\beta_s) = \frac{(\varepsilon/\rho_b)_f}{(\varepsilon/\rho_b)_0} = \frac{(E_{\mathrm{therm}}/A)_f}{(E_{\mathrm{TOT}}/A)}. \tag{2.16}$$

The index 0 indicates the initial fireball conditions, while f denotes parameters at freeze-out (i.e. at temperature T_f).

2.3.2 Freeze-out at constant global time. A constant-global-time hypersurface is defined by $\partial\sigma^0/\partial r = 0$ in which case the conservation laws take on the more convential form [1]

$$A = 4\pi \int_0^{R_f} \gamma\rho_b r^2 dr = 4\pi R_f^3 \rho_{b,f} \int_0^1 \frac{\xi^2 d\xi}{\sqrt{1-\beta_s^2\xi^{2n}}}, \tag{2.17}$$

$$E_{\mathrm{TOT}} = 4\pi \int_0^{R_f} [\gamma^2(\varepsilon + P) - P] r^2 dr$$

$$= 4\pi R_f^3 \left[(\varepsilon_f + P_f) \int_0^1 \frac{\xi^2 d\xi}{1-\beta_s^2\xi^{2n}} - \frac{P_f}{3} \right] \tag{2.18}$$

Now constancy of ε, P, ρ_b, T as well as the parametrization of the velocity profile are understood at constant global time. Here it is easer to first obtain β_s from the total energy per baryon E_{TOT}/A (R_f drops out from the ratio), and then insert the result into (2.17) and solve for R_f.

2.3.3 More realistic freeze-out surfaces. In [12, 57] we have studied the shape and properties of freeze-out surfaces resulting from the freeze-out criterium (2.7) when using more realistic, smooth initial transverse density and temperature profiles. We found the quite surprising result that (2.7) also in this case automatically leads to freeze-out surfaces which have a rather well-defined temperature and flow velocity in the sense that the bulk of the matter decouples with more or less the same T_f and $\langle\beta\rangle$. Although in this case most of the particles emerge from the time-like sections of the freeze-out surface, the resulting particle spectra show small deviations from the ones calculated in this paper (using the less physical freeze-out surfaces of Sects. 2.3.1/2), and only in the low-m_T-region $m_T < 400$ MeV. In the following sections this region will, therefore, always be discussed separately from the rest of the spectrum. The full analysis of all the spectra using the realistic freeze-out surfaces of [12] is not yet complete and will be published separately [57].

3 Transverse mass spectra

For fixed initial values $\varepsilon_0, \rho_{b,0}$ (or, equivalently, a fixed pair of parameters E_{TOT}/A, S/A) the freeze-out temperature T_f and the corresponding value of β_s have to be determined iteratively: for each new guess for T_f one calculates from the EOS at the given value of S/A the quantities $\varepsilon_f, \rho_{b,f}, P_f$, then from (2.12/13) resp. (2.17/18) R_f and β_s such that the time scales (2.8/9) can be evaluated and the freeze-out criterion (2.7) can be checked.

Once the correct freeze-out parameters for a specific particle species have been found, their energy spectrum is in our model given by a local thermal distribution with the freeze-out temperature T_f, boosted by the local velocity field $\beta(r, T_f)$. Thus, with $n = 2$ already fixed (see above), *three parameters determine the shape of the spectrum:* the particle mass, the freeze-out temperature T_f, and the surface velocity at freeze-out, $\beta_s(T_f)$. The general expression is [27]

$$E\frac{d^3N}{dp^3} = \frac{d^3N}{2\pi dy p_T dp_T} = \frac{g}{(2\pi)^3}\int_{\sigma_f} e^{-(\bar{E}-\mu)/T} p^\mu d\sigma_\mu, \tag{3.1}$$

(g is the spin-isospin degeneracy factor), where $\bar{E} = p^\mu u_\mu$ is the particle energy measured in the local fluid frame. In this expression we have already used the Boltzmann approximation which is in most cases adequate; generalized expressions containing also quantum statistical effects have been derived in [28, 12].
With

$$\bar{E} = p^\mu u_\mu = \gamma(E - \boldsymbol{\beta}\cdot\mathbf{p}) = \gamma(E - \beta p\cos\theta), \tag{3.2}$$

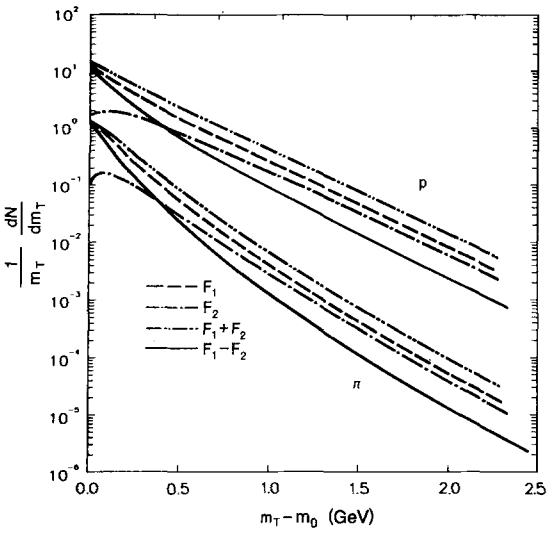

Fig. 1. The various contributions to the transverse mass spectrum $(1/m_T)dN/dm_T$ for pions and protons. (The absolute normalizations for each particle are arbitrary, by the relative normalization between the F_i is correct.) The freeze-out parameters correspond to the last line in Table 1a

where θ is the angle between the direction of observation (i.e. the direction of **p**) and the flow velocity of the fluid element, and from (2.4)

$$p^\mu d\sigma_\mu = \left(E - p\frac{\partial\sigma^0}{\partial r}\cos\theta\right) r^2 dr d(\cos\theta) d\phi, \tag{3.3}$$

we can easily do all the angular integrals. After also integrating over rapidity, we obtain for spherical expansion the general form of the p_T-spectrum

$$\frac{dN}{p_T dp_T} = \frac{ge^{\mu/T}}{\pi}\int dy \int_0^R r^2 dr E e^{-\gamma E/T} \left[\frac{\sinh\alpha}{\alpha} + \frac{T}{\beta\gamma E}\frac{\partial\sigma^0}{\partial r}\left(\frac{\sinh\alpha}{\alpha} - \cosh\alpha\right)\right] \tag{3.4}$$

where $\alpha = \beta\gamma p/T$, and for all parameters their freeze-out values are understood.

For final evaluation energy and momentum in the integrand have to be rewritten in terms of rapidity y and transverse mass m_T (or momentum p_T). We find

$$\frac{dN}{p_T dp_T} = \frac{dN}{m_T dm_T} = \frac{gR^3 e^{\mu/T}}{\pi}(F_1(m_T) - F_2(m_T)), \tag{3.5}$$

where (with $\bar{m}_T = \gamma m_T/T$)

$$F_1(m_T) = m_T \int dy \cosh y \int_0^1 \xi^2 d\xi e^{-\bar{m}_T \cosh y}\frac{\sinh\alpha}{\alpha}; \tag{3.6}$$

$$F_2(m_T) = T\int dy \int_0^1 \xi^2 d\xi \frac{\partial\sigma^0}{\partial r}\frac{e^{-\bar{m}_T\cosh y}}{\beta\gamma}\left(\cosh\alpha - \frac{\sinh\alpha}{\alpha}\right). \tag{3.7}$$

One sees that $F_1(m_T)$ is the contribution from a hypersurface of constant global time (Sect. 2.3.2), while any local variations of the freeze-out surface due to $\partial\sigma^0/\partial r \neq 0$ (see Sect. 2.3.1) contribute to the spectrum via F_2. Even for a constant expansion velocity the two contributions have a different m_T-dependence [29], due to the two different Bessel functions $\sinh\alpha/\alpha = \sqrt{\pi/2\alpha}I_{1/2}(\alpha)$ and $\cosh\alpha - \sinh\alpha/\alpha = \sqrt{\alpha\pi/2}I_{3/2}(\alpha)$ entering the respective integrands: for example, at $y=0$, while $F_1(m_T)$ approaches for $p_T \to 0$ a constant limit, F_2 vanishes in this limit as $(p_T/T)^2$. For $\partial\sigma^0/\partial r > 0$ (as in the case of a constant local time freeze-out surface) the difference between these two cntributions leads to concavity of the combined spectrum in the region $p_T < T$. However, a more realistic treatment using smooth density profiles yields [12] freeze-out surfaces with $\partial\sigma^0/\partial r < 0$ (including timelike sections of the surface), and the same is true for hydrodynamical simulations if freeze-out at a critical energy or particle density is postulated [24, 28, 29]. In this case F_2 contributes with the opposite sign and, depending on the details of the rapidity average (for example whether one integrates over all y or only selects a small window around $y=0$), the resulting spectra may tend to be slightly convex in the small-p_T ($p_T < T$) region [29]. To what extend this really happens will be discussed in Fig. 2. Please note that this effect has practically no influence on the slope in the medium- and large-p_T region ($p_T > T$).

Figure 1 shows an example of this for a freeze-out surface of constant local time, i.e. $\partial\sigma^0/\partial r = \beta(r)$. The spectrum is integrated over rapidity through the interval $-1.6 < y_{\text{c.m.}} < 1.6$; as a result the contribution F_2 does no longer vanish at $p_T = 0$ as is the case at $y=0$ for spherical geometry (see Fig. 2a) and at any y for a cylindrial geometry with longitudinal boost-invariance [29]. The solid line shows the difference $F_1 - F_2$ which describes the full spectrum for constant-local-time freeze-out; compared to F_1 alone which describes constant-global-time freeze-out, a slight enhancement of the concavity of the spectrum for small m_T is observed. The combinatin $F_1 + F_2$ (dashed-dotted line) indicates qualitatively the behaviour expected for a more realistic freeze-out suface which, according to the discussion above, has negative $\partial\sigma^0/\partial r$. Here only for pions a slight tendency towards convexity at small m_T is observed, in contrast to the boost-invariant cylindrical case studied in [29], where the vanishing of F_2 at $m_T = m_0$ leads to a much stronger flattening of the combination $F_1 + F_2$ in this region.

For $m_T - m_0 > 0.2$ GeV both combinations, $F_1 - F_2$ and $F_1 + F_2$, show concavity, the pions more so than the protons. This is different from the behaviour of thermal radiation at constant temperature. The origin of this concave curvature is analyzed in Fig. 2. We plot the various contributions to the spectrum $(1/m_T^{3/2})dN/dm_T$ (with the additional factor $m_T^{-1/2}$ extracted to facilitate comparison with thermal radiation) for pions, kaons and protons for different dynamical assumptions and cuts.

Figure 2a shows the spectra at $y=0$ for a spherical shell of temperature $T = 110$ MeV, expanding with constant velocity $\beta = 0.45$. The contributions F_1, F_2, and $F_1 - F_2$ (see (3.5–7)) are shown separately. (While the relative normalizations for F_1, F_2, and $F_1 - F_2$ are correct, the total spectra $F_1 - F_2$ for each particle species have been arbitrarily normalized to 1 at $m_T = m_0$. This facilitates the comparison of slopes.) The (arbitrarily normalized) purely thermal radiation spectrum is integrated over y

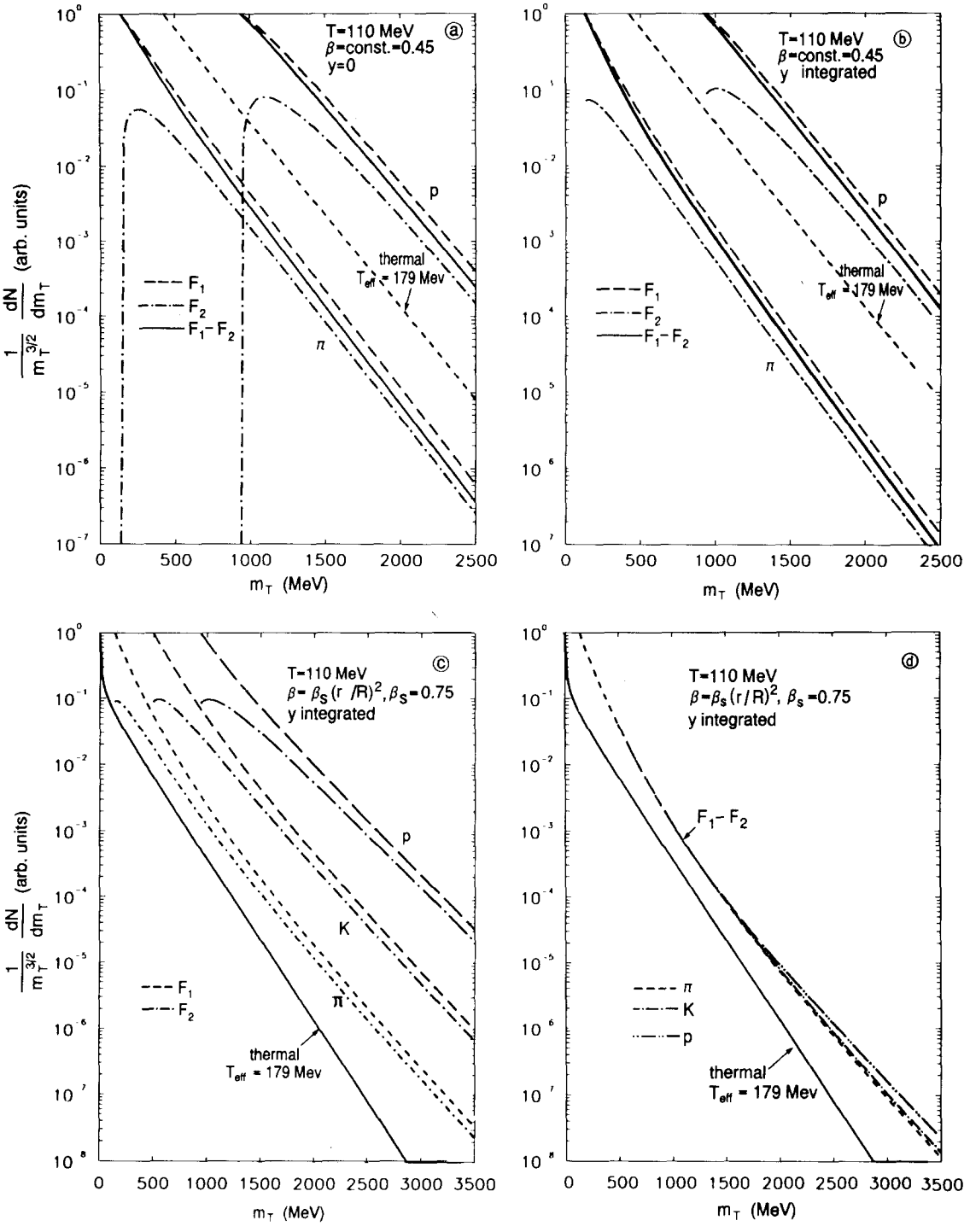

Fig. 2a–d. The various contributions to the transverse mass spectrum $(1/m_T^{3/2})dN/dm_T$ for different dynamical assumptions. All spectra $F_1 - F_2$ have been arbitrarily normalized to 1 at $m_T = m_0$, and the relative normalization of the F_i is exact. See detailed description in text

and has been calculated for an effective temperature corresponding to a blueshift of the true one by the absolute value of the flow velocity, $T_{\text{eff}} = T\sqrt{(1+\beta)/(1-\beta)}$. One sees that on a rough scale all contributions to the spectra approach the same slope at large m_T corresponding to this blueshifted temperature. Looking in more detail one realizes that they stay a little steeper, due to contributions from volume elements with longitudinal flow components whose transversal blueshift factor is smaller than the maximum one reached by volume elements whose flow points purely in the transverse direction. (This deviation from the aysmptotic slope with maximum blueshift is somewhat stronger in Fig. 2b where the spectrum is integrated over y which gives more weight to contributions from longitudinally moving volume elements.) At small m_T the global-time contribution F_1 turns slightly concave for pions, but has a convex shape for protons. Kaons lie in between. The convexity for

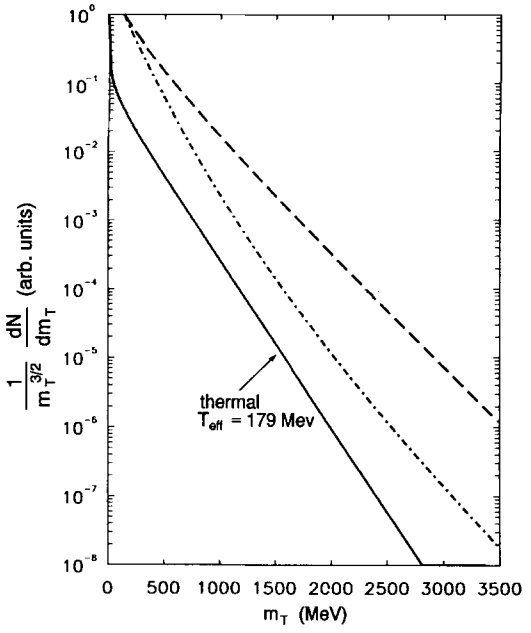

Fig. 3. Transverse mass spectra for thermal radiation without collective flow, but with variable temperature. See description in text

protons is nearly gone in the local-time spectrum $F_1 - F_2$, while the concavity of the pion spectrum is enhanced, in agreement with our above discussion.

For very large constant expansion velocities ($\beta > 0.65$) we found it possible to produce a small dip in the proton spectrum near $m_T = m_p$ and thus a peak in the m_T-spectrum [30]; however, this peak weakens with integration over y and usually vanishes once the spectrum is integrated over a realistic velocity profile.

Figure 2b shows the same spectra as Fig. 2a, but now integrated over y. The convexity of the proton spectrum becomes less pronounced, while the concavity of the pion spectrum gets slightly stronger.

In Fig. 2c, d we additionally integrate the spectrum over a parabolic radial flow velocity profile with the surface velocity chosen such that the same average flow of $\langle\beta\rangle = 0.45$ is recovered. We thereby reproduce the spectra shown in Fig. 1. Now we observe strong concavity in all global-time spectra F_1, and this feature is not qualitatively affected by the F_2 contribution. The asymptotic slopes now are much flatter than expected from a blueshifted temperature calculated with the average flow velocity; they correspond more closely to a blueshift factor calculated with the larger surface velocity β_s. Thus in the large-m_T tail of the distribution the fast expanding outer shells of the fireball dominate. Hence the strong concavity is primarily due to the fact that different shells with different flow velocities contribute different effective temperatures. Figure 2d shows that if the spectra from different particles are normalized onto each other, a nearly universal curve is obtained, with only small differences due to the different masses. The different average slopes obtained for different particles [1, 12] in a fixed internal of p_T (or of transverse kinetic energy $m_T - m_0$) are just a reflection of the intrinsic concave curvature of this universal curve: small-p_T protons probe larger values of m_T than small-p_T pions and thereby a region of flatter slope.

In Fig. 3 we investigate to what extent we can simulate the curvature in the spectra of Figs. 1, 2d (caused by the parabolic velocity profile) by thermal emission without any flow at all, but with a varying temperature. The solid line shows for comparison the radiation spectrum for a constant temperature $T_{0.45} = 179$ MeV (which corresponds to a radiation temperature $T = 110$ MeV blueshifted by an average $\langle\beta\rangle = 0.45$), i.e. $dN/(m_T^{3/2} dm_T) \sim \sqrt{m_T} K_1(m_T/T_{0.45})$. The dashed line shows an integration with constant weight of thermal contributions in the interval $T_1 \leqq T \leqq T_2$, where $T_1 = T_f = 110$ MeV and $T_2 = T_{0.75} = 291$ MeV (corresponding to a radiation temperature $T = 110$ MeV blueshifted by the surface velocity $\beta_s = 0.75$), i.e. $dN/(m_T^{3/2} dm_T) \sim \sqrt{m_T} \int_{T_2}^{T_2} K_1(m_T/T) dT$. Finally, the dash-dotted line shows an integration over the same interval, but with a variable weight: $dN/(m_T^{3/2} dm_T) \sim \sqrt{m_T} \int_{T_1}^{T_2} a^{(T-T_1)/(T_2-T_1)} K_1(m_T/T) dT$, with $a = 3 \cdot 10^{-4}$.

While the straightforward integration over temperatures within reasonable intervals always reproduces spectra which are nearly exponential and very similar to simple radiation spectra (although with a different effective temperature), a reasonable reproduction of the flow spectra of Fig. 2d has been achieved by the dash-dotted curve using a rather strange-looking weight-function which strongly suppresses the contributions from high temperatures relative to those from low-temperatures. This could be the situation in a system which is expanding only longitudinally, with a time dependence such that the systems cools very fast initially, but rather slowly towards the end. It is not clear to us whether such a dynamical picture may be realistic.

4 Results: the experimental evidence for collective flow

4.1 Analysis of CERN data

In [1] we used the model described above to obtain an excellent fit to the π^0 transverse momentum spectra [2] from central O + Au collisions at 200 A GeV. Since the fireball radius scales out from the spectrum and thus does not affect its shape, but only its normalization (which is anyway theoretically uncertain since it strongly depends on the degree of chemical equilibrium reached in the collision), it only enters the final results in a very weak way through the rarefaction time scale (2.9) in the freeze-out criterion. Thus it essentially has to be determined independently (for example by 2-pion interferometry [31]). If we leave it as a free parameter, we obtain from our fit to the π^0 spectrum a whole set of possible initial conditions $(\varepsilon_0, \rho_{b,0})$ (see Tables 1 and 2 [26, 32]). It is interesting to note [1, 12] that they all correspond roughly to the same initial thermal energy of the fireball, i.e. E_{TOT}/A, and only differ in its specific entropy. Thus, for a given spectral shape, fixing the fireball radius is in our model equivalent to fixing S/A.

a

Initial conditions					Freeze-out for nucleons			Freeze-out for K^+ mesons		
ε_0	ρ_0	T_0 MeV	S/A	R_0 *fm*	T_N MeV	R_N *fm*	$\beta_{s,N}$ *c*	T_{K^+} MeV	R_{K^+} *fm*	β_{s,K^+} *c*
1.0	0.64	150	7.52	2.9	110	4.6	0.74	140	3.2	0.38
2.0	1.33	154	6.08	2.3	106	3.8	0.77	137	2.7	0.47
3.0	2.03	156	5.42	2.0	103	3.5	0.79	133	2.0	0.52

b

Initial conditions					Freeze-out for nucleons			Freeze-out for K^+ mesons		
ε_0	ρ_0	T_0 MeV	S/A	R_0 *fm*	T_N MeV	R_N *fm*	$\beta_{s,N}$ *c*	T_{K^+} MeV	R_{K^+} *fm*	β_{s,K^+} *c*
1.0	0.58	161	8.62	3.0	112	4.7	0.72	148	3.3	0.38
2.0	1.27	164	6.65	2.3	108	3.7	0.72	143	2.7	0.45
3.0	1.94	167	5.90	2.0	105	3.4	0.74	140	2.4	0.50

Table 1 a, b. Different initial conditions of the fireball which fit the measured pion spectra in central 200 A GeV O + Au collisions, and the corresponding freeze-out values for nucleons and K^+ mesons. **a** Freeze-out at constant local time; **b** freeze-out at constant global time

a

Initial conditions					Freeze-out for nucleons			Freeze-out for K^+ mesons		
ε_0	ρ_0	T_0 MeV	S/A	R_0 *fm*	T_N MeV	R_N *fm*	$\beta_{s,N}$ *c*	T_{K^+} MeV	R_{K^+} *fm*	β_{s,K^+} *c*
1.0	0.62	153	7.79	3.4	109	5.6	0.78	141	3.8	0.42
2.0	1.29	161	6.47	2.7	108	4.7	0.80	140	3.2	0.51
3.0	1.94	167	5.90	2.3	107	4.2	0.83	140	2.9	0.57

b

Initial conditions					Freeze-out for nucleons			Freeze-out for K^+ mesons		
ε_0	ρ_0	T_0 MeV	S/A	R_0 *fm*	T_N MeV	R_N *fm*	$\beta_{s,N}$ *c*	T_{K^+} MeV	R_{K^+} *fm*	β_{s,K^+} *c*
1.0	0.62	151	7.61	3.4	104	5.2	0.70	137	3.8	0.39
2.0	1.31	157	6.24	2.7	102	4.3	0.72	135	3.1	0.48
3.0	1.99	161	5.63	2.3	99	3.9	0.74	132	2.8	0.52

Table 2 a, b. Different initial conditions of the fireball which fit the measured pion spectra in central 14.6 A GeV/c Si + Au collisions, and the corresponding freeze-out values for nucleons and K^+ mesons. **a** Freeze-out at constant local time; **b** freeze-out at constant global time

In practice we have for concreteness assumed that the initial fireball radius is equal to the transverse radius of the (smaller) projectile; i.e. for O + Au, Si + Au, and S + S collisions we took $R_0 = 2.5$, 3.0, and 3.1 fm, respectively. The consistency of this choice will have to be checked in the future by an independent determination of the specific entropy (e.g. from particle ratios [33]) or of the radius at freeze-out from 2-particle interferometry. According to the analysis of 2-pion correlation data by the NA35 collaboration there are indications for a very large transverse freeze-out radius (of order 5–6 fm in S + S collisions and up to 8 fm at midrapidity in O + Au collisions). Their fit, however, does not take into account the possible effects of a strong radial flow on the correlation function. Such an analysis should be performed before judging whether or not the considerably smaller freeze-out radii in our model (see Table 1) are inconsistent with the data.

It is surprising to find that all parameter sets in Tables 1 and 2 correspond in the initial state to nearly the same thermal energy per baryon, $\varepsilon_0/\rho_{b,0} = E_{\mathrm{TOT}}/A \simeq 1.5$ GeV/nuleon, independent of the beam energy. On the other hand, the initial states for O + Au and S + S collisions, which have approximately the same number of participants, correspond to different initial energy *densities* because in the S + S case we allow the participants to be spread over a large initial volume. This is definitely an artifact of our assumed spherical geometry; incomplete stopping will allow the baryon number to spread over a larger rapidity range, thereby reducing the initial baryon density. This dilution effect will be relatively stronger for the oxygen induced reactions. This will at the same time resolve another problem with our initial state parameters, namely that it is impossible to obtain with an initial energy per baryon of only 1.5 GeV

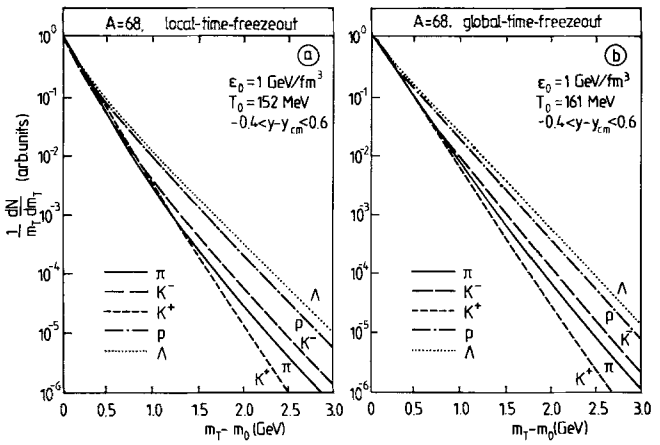

Fig. 4. **a** Transverse mass spectra for pions, kaons, protons, and Λ's in central 200 A GeV O + Au collisions, obtained from the parameter set in the Table 1a (constant-local-time freeze-out) interpolated to an initial radius $R_0 = 2.5$ fm. All the curves are arbitrarily normalized at $m_T = m_0$. **b** The same for the parameters of Table 1b (constant-global-time freeze-out)

a final pion to proton ratio of order 5 to 10 as observed in the S + S collisions near midrapidity [8]. As the initial energy density, temperature and pressure cannot become appreciably smaller than the values quoted in Tables 1 and 2, because such high values are needed to reproduce the flatness of the observed transverse mass spectra, the initial energy per baryon (and thus the specific entropy and the observed pion/baryon ratio) will increase by this mechanism. In this sense the estimated values for S/A from this work have to be considered as lower estimates. Indeed, independent analyses based [33] on measured particle ratios seem to point towards considerably larger values [34].

In Fig. 4a, b we show (for the two cases of constant-local-time and constant-global-time freeze-out) our theoretical curves obtained from a fit of the initial conditions to the pion data, as well as the predicted shapes for other hadron spectra. Except for the K^+ mesons, all hadrons shown freeze out essentially together, due to their strong coupling with each other via the nucleons which here form the dominant fraction of the particle density. Basically, since $\sigma_{\pi N}$ and $\sigma_{\bar{K}N}$ are resonance dominated in the momentum region of interest, while $\sigma_{\pi\bar{K}}$ is much smaller, the nucleons serve as a heat bath and their freeze-out temperature determines the freeze-out temperature also for the other particles. Only the K^+ mesons are different, since they have a very small interaction cross section (< 10 mb) with nucleons, and their (isospin averaged) interaction with the (in our applications) less abundant pions does not exceed 60 mb even in the peak of the rather narrow K^* (892) resonance [35]. Thus they freeze out considerably earlier (see Table 1). At this point the temperature is higher (which should lead to a flatter spectrum), but the flow is less developed (which counteracts this effect). The final result from our calculation here is a K^+ spectrum which for small p_T is marginally flatter than the K^- one, but nearly straight (i.e. thermal) due the small flow velocity. In contrast, the K^--spectrum is visibly curved as an effect of the stronger flow velocity at K^- freeze-out, leading to a flatter slope than the one of the K^+ mesons at large p_T. The cross-over point between the two slopes depends somewhat on which freeze-out surface is chosen and here lies in the region between $0.5\,\text{GeV} < m_T - m_0 < 1\,\text{GeV}$.

It should be kept in mind that this calculation was done with a hadron gas EOS and should thus not be confused with our earlier prediction [16] of a steepening effect of a QGP phase transition on the K^+ spectra. In [16] the initial conditions for a hadron gas EOS of the fireball were estimated from a compression shock calculation and corresponded to much higher initial temperatures. As a result the kaons froze out at a higher temperature, too, mainly because flow developed earlier, and the combination of these two aspects results in a K^+-spectrum which in the case of a hadron gas EOS was always flatter than the K^- one. This led us to suggest that the steeper K^+ slope from a hadronizing QGP (where kaon freeze-out occurred at a lower temperature which actually was quite similar to the K^+ freeze-out temperature obtained here with a hadron gas EOS) could be a unique signature for a QGP phase transition and the cooling effects [16] of quark–gluon plamsa formation. We see now that the experimental data appear to drive us towards such a rather cool initial state anyway, leaving apparently no more room for a clear distinction between the two scenarios. Of course, this should be further studied by comparing the analysis of the present paper with one which allows for QGP or mixed phase formation. Furthermore, the results could also drastically change if, in the course of relaxing the spherical symmetry constraint, initial conditions with smaller baryon density, but higher temperatures should also prove consistent with the data. Obviously, this is point for further research, and it makes also the experimental study of the kaon spectra very interesting.

While the small difference between K^+ and K^- spectra, at least in the low-p_T region, is very hard to measure and requires very high kaon statistics (first experimental data from the E802 spectrometer will be discussed below), we see in Fig. 4 that the predicted splitting between the slopes of pions, protons, and Λ's due to the flow effects is much stronger and thus easier to test. This is done in Fig. 5, using the pion, $K^0_s, \bar{\Lambda}$ and $\bar{\Lambda}$ m_T-spectra from 220 A GeV O + Au collisions [3, 7].

In Fig. 5a we show our fit to the pion spectra together with the very high statistics data from WA80 [2] (which were the basis of our fit) and the negative particle spectra from NA35 [3] (which have a small $O(10\%)$) kaon contamination). The fit with a constant-global-time freeze-out surface appears to be somewhat better than the one corresponding to constant local time; however, it should be noted (see Table 1) that the two fits correspond to slightly different initial conditions, resulting in somewhat different freeze-out temperatures and flow velocities. While the fit is excellent for the WA80 data which do not give information below $p_T = 400$ MeV/c but reach out to transverse momenta of nearly 3 GeV/c, the NA35 data seem to overshoot the theoretical curve at very small transverse momenta $p_T < 200$ MeV/c. Given the fact that more realistic freeze-out surfaces rather tend

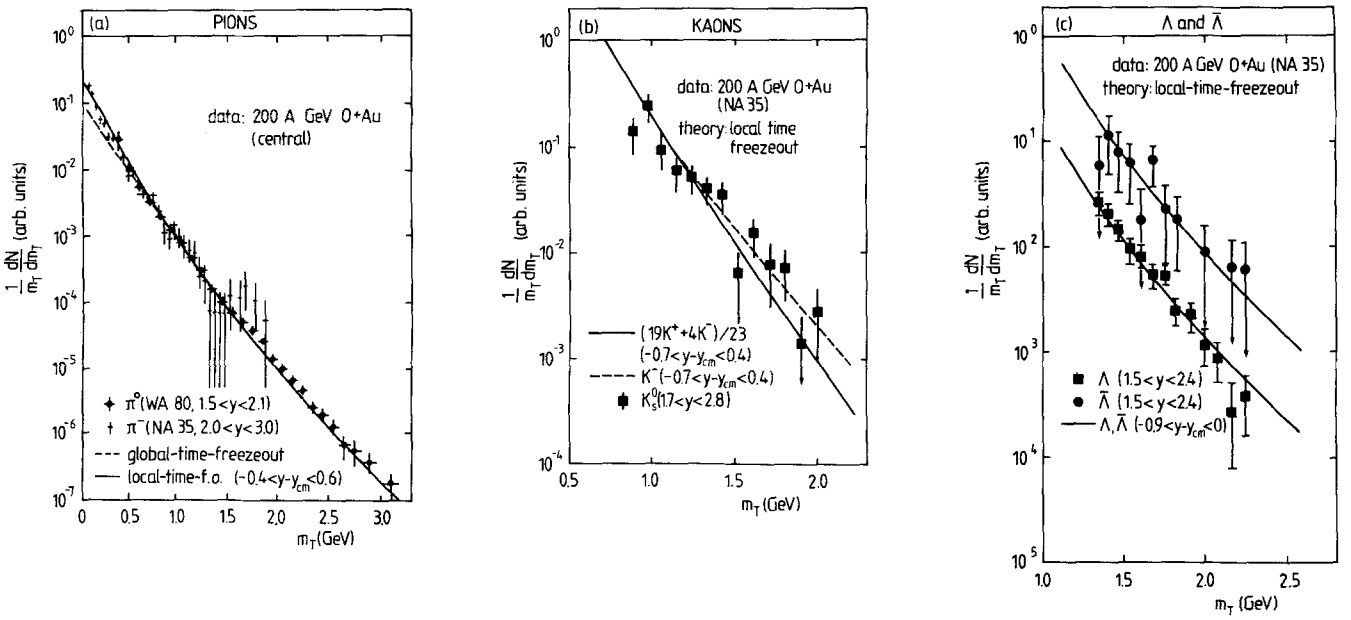

Fig. 5. a Transverse mass spectra for neutral and negative pions from central 200 A GeV O + Au collisions by WA80 [2] and NA35 [3, 8]. These data were used to obtain the model parameters in Table 1. The solid (dashed) curves are fits using a local-time (global-time) freeze-out surface. The relative normalization of data and theory is arbitrary. **b, c** Transverse mass spectra for K_s^0, Λ, and $\bar{\Lambda}$ [7]. The curves are those from Fig. 4a, but the corresponding ones from Fig. 4b are hardly distinguishable

to flatten the theoretical spectra in this region (see Sect. 2.3), our model is not able to reproduce such a behaviour, which would thus require a different mechanism in the very-low p_T region. One might think of a cold target spectator contribution, but since the data are selected for a central rapidity slice where the total pion multiplicity is very large, any target spectator component leaking into this y-interval would be much smaller and make a small correction to the spectrum.

In Fig. 5b the predicted shape for the $K_s^0 = (K^0 + \bar{K}^0)/2$ is shown together with the data [7] (see also J. Harris [8] for a similar comparison). We show two curves for comparison: the flatter one (labelled K^-) corresponds to $\bar{K}^0$ only, the steeper one to a mix of K^0 and $\bar{K}^0$ according to the relative abundances of kaons and anti-kaons measured in the Brookhaven E802 experiment (see Sect. 4.2). Since we do not know for the NA35 experiment which fraction of K_s^0 stems from K^0 and $\bar{K}^0$, respectively, and the two contribute differently to the spectrum due to the predicted different freeze-out temperatures, it is hard to say which of the two theoretical curves is more realistic. The better *fit* is obviously obtained by the curve labelled K^-, i.e. by assuming that the K_s^0 mesons stem from neutral kaons which froze out at a late stage together with the pions, protons and hyperons, rather than at any early stage as predicted for the K^+.

Therefore, the situation with kaons is not at all clear. Further indications for a possible discrepancy with our theory arise from preliminary results from the HELIOS spectrometer [9, 36] which identified K^+ and K^- from 200 A GeV S + W collisions in the target fragmentation region $1 \leqq y \leqq 1.3$, $0.5\,\text{GeV} < m_T < 0.7$ GeV. These data show a slope for the K^- m_T-spectrum which is slightly steeper than the pion one in the same m_T region, while the K^+ slope is considerably flatter than the pion one. To the extent that the p_T coverages overlap, these findings are in qualitative (and within errors even quantitative) agreement with the results from the E802 collaboration [11] at much lower beam energies (14.5 A GeV). Although qualitatively these features are also reproduced by our theoretical curves (at least in this low-p_T region, see Fig. 4), in quantitative terms the measured K^+ spectrum appears to be significantly flatter than predicted. The fact that the K_s^0 spectra from NA35 (even if they come from a more central rapidity slice) show the same tendency also at larger m_T goes in the same direction. More data with better statistics over a larger m_T region will be needed to settle this question.

Fig. 5c shows the Λ and $\bar{\Lambda}$ spectra from the O + Au collisions [7] together with our prediction from Fig. 4. The theoretical curves for Λ's and $\bar{\Lambda}$'s are identical, since we assumed simultaneous freeze-out for both species. The agreement with the data is quite good and demonstrates that hyperons have indeed a flatter spectrum than pions in the measured range of transverse kinetic energies $m_T - m_0$ or, in other words, that the "universal" m_T-spectrum shown in Fig. 2d is indeed curved.

It is worth noting that even when using the formulae (3.5–7) from our model to analyze the data, such an immediate success is not guaranteed if one does not properly include the freeze-out concept. In other words, doing a free fit of T_f and β_s to the spectrum of a single species of hadrons without checking the compatibility of this pair of parameters with the freeze-out criterion will in general lead to failure with other particles. In particular, if e.g. in the pion spectrum a hard scattering component at large p_T becomes visible (as is, for example, the case in peripheral nuclear [2] or proton–nucleus collisions [6]), a l.m.s. fit of the spectrum inevitably leads

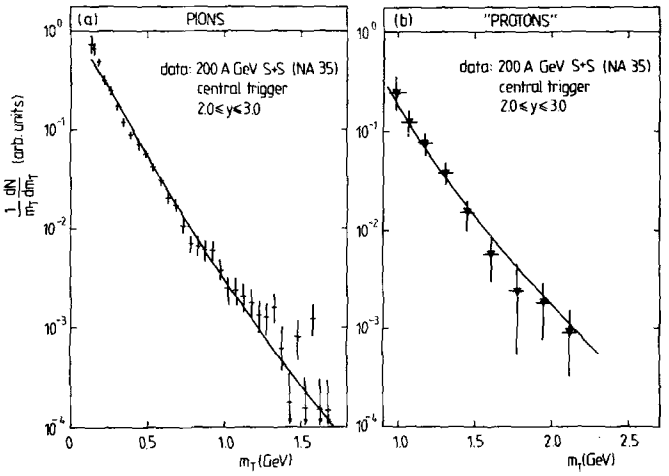

Fig. 6 a, b. Transverse mass spectra for negative pions **a** and for "protons" (i.e. positive minus negative tracks) from central 200 A GeV S + S collisions [8a]. Theoretical curves are from Fig. 4a

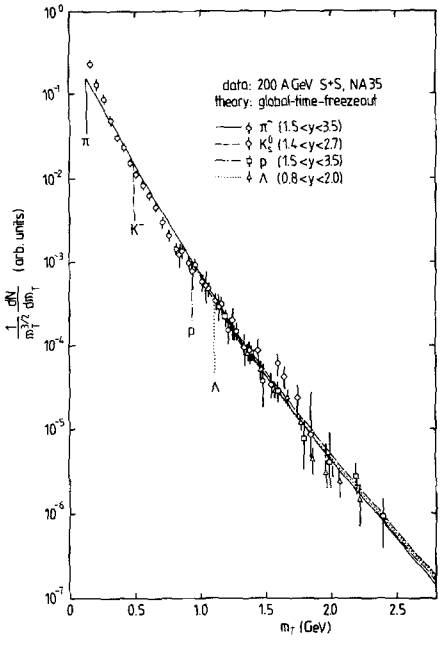

Fig. 7. $(1/m_T^{3/2})dN/dm_T$ for pions, kaons, "protons", and Λ's from central 200 A GeV S + S collisions [8c]. The initial state parameters for the theoretical curves are as in Fig. 4b. Since the y-distributions predicted by the spherical model do not agree with the data (see Fig. 8), the theoretical curves have been integrated over y. Globally the fit to the pion spectrum shown here (global-time freezeout) is a little better than the one in Fig. 6 (local-time freezeout), however, the low-p_T "anomaly" appears more significant

to a combination of low T_f and large β_s (the latter being enforced by the strong bending of the spectra at large p_T which however in this case has nothing to do with collective flow); the high β_s would in turn influence the heavier Λ's very strongly and lead to a much too flat predicted spectrum.

Several studies [37, 38] have shown that in a free fit to a given spectrum the compatible values of T and β are anticorrelated, and the fit quality may allow for a rather wide variation (high-T, low-β combinations giving similar quality fits as low-T, high-β ones). In contrast, the freeze-out criterion provides a direct correlation between these parameters: high flow values lead to earlier freeze-out (i.e. at high T), and vice versa. Combining both pieces of information considerably restricts even for a single particle species the allowed range of parameter pairs, and a careful comparison with other particle species finally constrains the system completely.

The available particle spectra from 200 A GeV S + S collisions [8] can be fit by the same set of initial conditions (we only changed the initial fireball radius to the one for sulfur). Since in this case in central collisions all projectile and target nucleons are involved, the baryon number of the fireball is nearly identical to the O + Au case. Our results for pions and protons (experimentally obtained by subtracting all negative from all positive tracks [8] rather than direct identification) are shown in Fig. 6. Again the predicted flatter slope of the protons is borne out in the data.

In Fig. 7 we show the same data (with slightly different kinematic cuts [8c]), including also kaon and Λ data from the S + S system. We here chose to plot $(1/m_T^{3/2})dN/dm_T$ as in Figs. 2, 3 where we compared spectra with flow to purely thermal ones. One sees that in this representation, with the different spectra normalized onto each other at the point $m_T = m_0$, both the theory and the data lie rather well on a universal curve with concave curvature. In the data the curvature is clearly visible only up to $m_T \sim 1$ GeV (i.e. it is mostly due to the pions), while for larger m_T the data could also be well represented by a straight line with a slope parameter of about 200 MeV. It is clear that more data at larger values of m_T are required to settle the question of continuing concave curvature in the spectra and thus to clarify whether or not there is collective flow. Theoretically, it has to be studied whether there are other mechanisms, in particular in the pion channel which is mostly responsible for the apparent curvature, which can explain the nonthermal nature of their m_T-spectra. An analysis of resonance decay contributions to the spectra is under way; it appears that a large fraction of the low-p_T enhancement in the pion data, which we find so hard to fit by our flow hypothesis (see Figs. 6, 7), may be due to resonance decays from ω and ρ mesons [58].

Figure 7 clarifies why it was found in [37] that it is also possible to fit the proton and Λ^0 spectra by a purely thermal distribution with a single temperature (this is not possible for the pions). The resulting values for T are much higher than those obtained with the flow hypothesis and are different for different particle species; calculating for example a thermal pion spectrum with the apparent Λ temperature yields a much flatter spectrum than measured. Such different temperatures for pions, protons and Λ's are hard to understand theoretically, while the collective flow hypothesis yields a much more natural interpretation of the data with one single set of parameters.

In Fig. 8 we show that our spherical fireball picture fails to describe the longitudinal momentum distributions. The rapidity distribution from our flow model is even slightly narrower than a purely thermal one with an

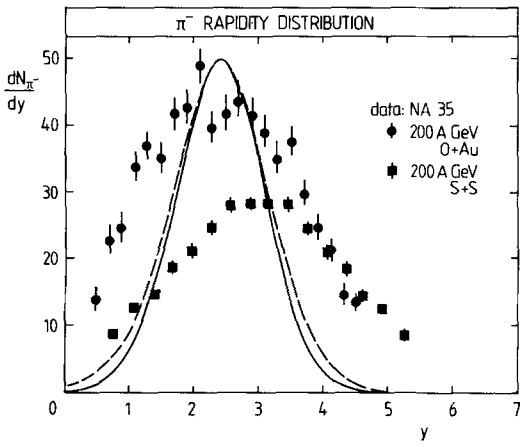

Fig. 8. Rapidity distributions for negative pions from central 200 A GeV O + Au and S + S collisions [3, 8]. The theoretical spectrum uses the parameters from Fig. 4 which fit well the m_T-spectra

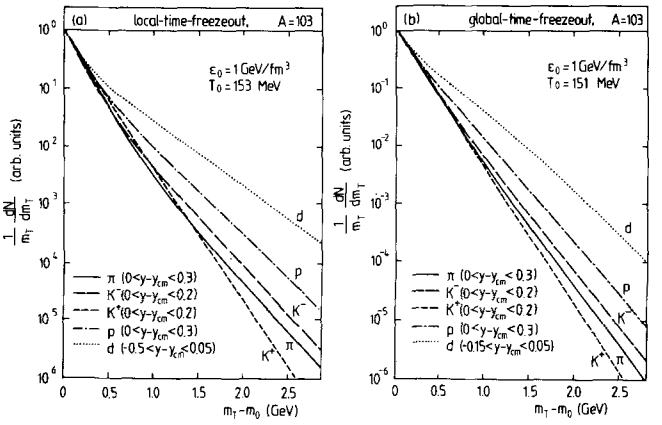

Fig. 9. a Transverse mass distributions for pions, kaons, protons, and deuterons in central 14.5 A GeV Si + Au collisions, obtained from the parameter set in Table 2a (constant-local-time freeze-out) for an initial radius of 3.0 fm. All curves are arbitrarily normalized at $m_T = m_0$. **b** The same curves for the parameter set in Table 2b (constant-global-time freeze-out)

effective temperature of 200 MeV (i.e. the asymptotic slope parameter in Fig. 7). Clearly the assumptions of spherical symmetry is too restrictive, and the much wider experimental rapidity distribution is an indication for much stronger flow occuring along the beam axis than in the transverse directions. We will present a combined analysis of both the transverse and longitudinal momentum distributions within a flow model with only cylindrical symmetry in a future paper.

The failure of the spherical model with respect to the rapidity distributions renders a quantitative interpretation of the initial state parameters ε_0, $\rho_{b,0}$ very dangerous: obviously, our analysis includes in the energy balance only the kinetic energy from transverse collective flow (which had to come from thermal energy density initially). If one interprets the measured rapidity distribution as evidence for even stronger collective flow in the longitudinal direction, and furthermore assumes that also this flow energy was at one point thermalized (Fermi–Landau model [15, 39]), one of course obtains much higher estimates for the initial energy densities [39, 40]. We will further discuss this issue in the conclusions.

4.2 Analysis of E802 data

The E802 collaboration has measured various particle spectra in central Si + Au collisions at 14.5 A GeV. In contrast to the situation at CERN, at this energy large target nuclei can stop the projectile completely [41, 42], leading to a very large baryon density in the collision zone. Hence this experiment is especially suitable for testing the idea [16] that if a baryon-rich QGP is formed, the inversion of K^+ and K^- slope parameters may signal the short-lived existence of a baryon-rich QGP. Even in the case that the collision is purely hadronic, the measurement of particle spectra for a large variety of hadron species will seriously test our model and the possible formation of a fireball during the collision.

When the measured m_T spectra of pions, K^+ and K^- mesons, protons, and deuterons were first presented [10], it was immediately noticed [43] that the data show qualitative agreement with the predictions from our above model. Furthermore, the y-dependence of the slope parameter extracted from the proton m_T spectra shows a behaviour compatible with that of protons isotropically emitted from a spherical fireball [10]:

$$T_{\text{eff}}(y) = \frac{T_{\text{eff}}(y_{\text{cm}})}{\cosh(y - y_{\text{cm}})}. \tag{4.1}$$

In this section we will now analyze these experimental findings in detail, following the same procedure as in the previous section, with a fireball containing $A_{\text{FB}} = 103$ baryons (see Sect. 2.1) and having the initial radius of the Si projectile.

Again we begin by determining a set of initial stage parameters such that after expansion and freeze-out the measured pion spectra are reproduced. The results are tabulated in Table 2 (Sect. 4.1). Once the initial state is thus fixed, the slopes of all other particle spectra are found to come out right without any adjustment of parameters.

The particle spectra obtained from the initial conditions in Table 2 are shown together in Fig. 9. Again the theoretical spectra are normalized arbitrarily, in order to concentrate on their shapes. There is a large difference between the slope parameters calculated for pions, protons and deuterons; the difference between pions and kaons is smaller, and the details also depend somewhat on the choice of freeze-out hypersurface. While for local-time freeze-out the K^+ spectrum is considerably flatter than the K^- one up to $m_T \simeq 1$ GeV, this is not the case for global-time freeze-out where the two slopes come out nearly equal in the low-m_T region while at large m_T the K^+ are steeper.

In [11] the m_T-spectra were fitted under the assumption of purely thermal radiation, with a Boltzmann distribution centered in the middle of the measured rapidity interval ($1.2 < y < 1.4$ for pions, kaons and protons) and not integrated over y. The data explore roughly the regions 0.2 GeV $< m_T - m_0 <$ 0.8 GeV for π^+ and π^-, $0 < m_T - m_0 < 0.5$ GeV for K^+ and K^-, and

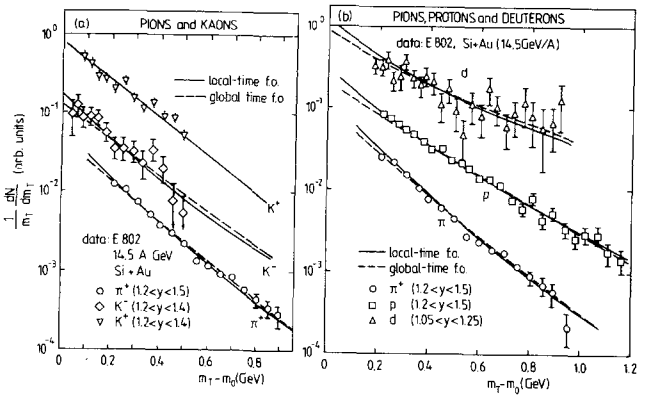

Fig. 10 a, b. Comparison of the theoretical curves in Fig. 9 with the E802 data. **a** Pions from [10] and kaons from [11]. For K^+ the results for local- and global-time freeze-out are indistinguishable. **b** Pions, protons, and deuterons from [10]. All normalizations are arbitrary

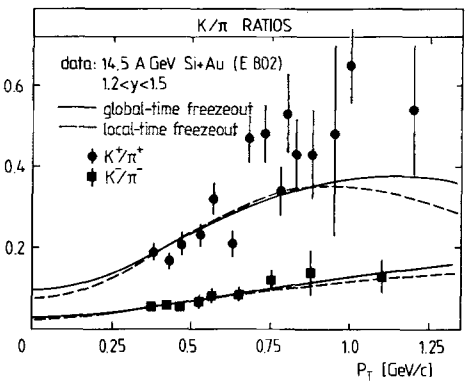

Fig. 11. K/π ratios as a function of p_T from the E802 experiment [10] and from our model. The theoretical curves are normalized to the measured integrated K/π ratios

$0 < m_T - m_0 < 1$ GeV for protons. In these regions the following effective temperatures were found: $T_{\text{eff}}(\pi^+) = T_{\text{eff}}(\pi^-) = 126 \pm 10$ MeV, $T_{\text{eff}}(K^-) = 140 \pm 25$ MeV, $T_{\text{eff}}(K^+) = 160 \pm 15$ MeV, and $T_{\text{eff}}(p) = 187 \pm 5$ MeV, corresponding to the pattern $T_{\text{eff}}(\pi) < T_{\text{eff}}(K^-) < T_{\text{eff}}(K^+) < T_{\text{eff}}(p)$. While for the pions the spectra for the two charge states are identical to high accuracy [11], this does not appear to be the case for the kaons. In Fig. 10 we show that, within the error bars, this pattern can be quantitatively reproduced by our model. Of course, the statistics on the kaons are not yet good enough to clearly say whether or not there is a difference in slope between the two charge states; within the errors, both our local-time and global-time freeze-out curves pass through the data. Still, there are indications for some small differences between the K^+ and K^- data, not only in abundance but also in the spectral shape; this is very interesting and should be further studied with higher accuracy.

In Fig. 10 we show our fit to the pion spectrum and the predicted spectra for the other particles together with the data. While the pion and kaon spectra are for all practical purposes parallel, and (in contrast to the pions at CERN energies) one cannot see a strong curvature within the measured m_T-ranges, the presence of the curvature is implicit in the different slopes seen for pions, protons and deuterons. This is very clearly demonstrated in Fig. 10b, which shows that the larger m_T, the flatter the spectra become, both in the flow model and in experiment.

That the deuterons show the flow so clearly may seem surprising at first sight, since they are only weakly bound and certainly will not exist as elementary particles in the hot fireball. Instead they will form by coalescence of protons and neutrons at freeze-out. However, the weak binding of those two nucleons in the deuteron requires a very small coalescence radius in momentum space, such that the nucleon momenta (which carry both the thermal and flow information) add up to a deuteron momentum which is exactly as it would have been for an elementary deuteron in the same temperature and flow velocity field. This feature was observed previously at the BEVALAC (for reviews see [44]), where the coalescence model proved very successful in explaining the properties of small nuclear fragments. A calculation of the deuteron spectra within a relativistic coalescence model applicable to BNL and CERN energies is under way.

The kaon data of Fig. 10a have also been presented in a different way [10] which has given rise to some excitement: Fig. 11 shows the kaon-to-pion ratios as functions of p_T. Both ratios rise with p_T, but the slope is significantly steeper for K^+/π^+ than for K^-/π^-. On the other hand, the π^+/π^- ratio is 1 independently of p_T [10, 11]. Also shown in Fig. 11 are the predictions from our model. For this the theoretical spectra were first reevaluated as a function of p_T, then normalized relative to each other according to the measured integrated K/π ratios and finally divided by each other. The second step is necessary since our model implicitly assumes chemical equilibrium all the way until thermal freeze-out, and thus we did not a priori expect very good agreement of our integrated K/π ratios with the experimental ones. However, the deviations are surprisingly small: we obtain $K^+/\pi^+ = 0.24$ and $K^-/\pi^- = 0.056$ for local-time freeze-out ($K^+/\pi^+ = 0.31$ and $K^-/\pi^- = 0.045$ for global-time freeze-out), while the experimental values [11] are $K^+/\pi^+ = 0.192 \pm 0.03$ and $K^-/\pi^- = 0.036 \pm 0.008$. Thus the measured integrated ratios, which are different from those in pp collisions at similar energies [45, 10, 11], indicate a strong approach towards chemical equilibrium even in the strange sector. This was also found in [34], and similar indications come from the strong rise with collision centrality of the $\Lambda, \bar{\Lambda}$, and K^0_s-to-charged multiplicity ratios found by NA35 [46], and by the enhancement of ϕ meson production in central O + U and S + U collisions found by the NA38 collaboration [47] (for an analysis see [48]).

We see in Fig. 11 that the p_T-dependence of the K^-/π^- ratios is very well described by our model, while we do not quite reproduce the very strong rise in the K^+/π^+ ratio. This again indicates (as for the kaons at CERN energies) that the measured K^+ spectra are somewhat flatter than predicted. Data for larger m_T and with better statistics would be very valuable for further illuminating this potential problem.

In Fig. 12 we show the rapidity dependence of the

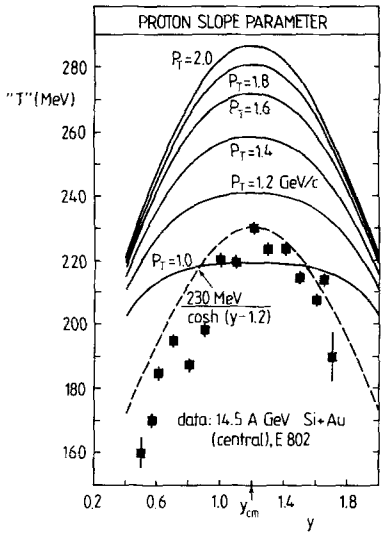

Fig. 12. Proton slope parameters as a function of rapidity. The data are experimental results from a straight exponential fit within the acceptance region [10], while the theoretical curves show the local slope parameters for a series of p_T values

slope parameters for the proton transverse mass spectrum, $(1/m_T)dN_p/dm_T$. The data points [10] correspond to a straight exponential fit $\sim \exp[-m_T/T_{\text{eff}}]$ of this quantity within the acceptance region. The dashed line is a naive fit [10], assuming a non-expanding spherical fireball moving with $y_{\text{cm}} = 1.2$ and radiating with a temperature of 230 MeV. The solid lines are the predictions of our flow model, for an expanding fireball (with initial conditions given by the first line in Table 2a) located at $y_{\text{cm}} = 1.2$ (i.e. at the peak of the data points). New data on the rapidity distributions of pions from the E802 experiment [11] show that they peak at a somewhat larger value, $y_{\text{peak}} = 1.46$, and that (in contrast to the CERN data, see Fig. 8) they can be successfully fit by a spherical fireball model with the fireball located at y_{peak}. (Although in [11] the fireball was assumed not to expand collectively, an expanding fireball would have done an equally good job since the rapidity distributions are nearly identical in both cases, see Fig. 8.) That the slope parameters in Fig. 12 peak at a smaller y (this is also true for the pion slope parameters, see [11]) may be an artifact of the spectrometer acceptance. This can be seen from Fig. 12 in the following way:

Since in our flow model the proton spectra show a concave curvature, the effective slope parameter of the spectra depend on p_T, with smaller values (steeper spectra) at small p_T and larger values (flatter spectra) at large p_T. [The curvature is strongest in the central rapidity slice (i.e. in the fireball c.m.) and becomes weaker in the forward and backward rapidity slices.] Since the E802 spectrometer is sensitive [11] only to very small values of p_T in the forward direction, the effective slope is there dominated by the steeper low-momentum part of the spectrum. On the other hand, in the backward region the p_T-acceptance ranges to much larger values, thereby probing also the flatter parts of the spectrum. This leads to a systematic shift of the maximum of the slope parameters towards smaller values of y. In Fig. 12 we have not accounted for this shift because this would have required a folding of our model calculations with the experimental acceptances. We believe that the largest part of the difference in shape between the data and our curves is due to such acceptance corrections and the resulting y-dependence of the p_T-averaging process used in fitting the slopes.

In order to test our prediction of curved spectra as a result of transverse flow, i.e. a p_T- and y-dependence of the slope parameters ("effective temperatures"), we suggest taking data with higher statistics and plotting the slope parameters for various p_T bins as a function of y as done in Fig. 12.

5 Conclusions

We have analyzed the particle spectra measured in central 200 A GeV O + Au and S + S collisions and in central 14.5 A GeV Si + Au reactions within a thermal fireball model with collective expansion flow. After reviewing the model and deriving general expressions for hadronic momentum spectra from thermalized systems with spherical expansion velocity profiles, we analyzed in some detail the influence of the shape of the freeze-out hypersurface and of the flow velocity profile on the spectral shapes. Finally in Sect. 4, we performed a quantitative description of the available data within the model.

Although in the practical calculations shown here the expansion geometry was restricted to spherical symmetry, we found that the model describes surprisingly well all the transverse aspects of the collision. For all collision systems which we studied, our model quantitatively describes the complete set of available hadronic m_T-spectra with a single pair of initial fireball parameters ε_0, $\rho_{b,0}$ for the hot zone formed by the participants of the collision. We find that, as a function of m_T, and after suitable normalization, the spectra for different hadronic species lie on a universal curve which has significant concave curvature, i.e. which possesses a flatter slope at large m_T than at small m_T. This translates into flatter spectra for heavier hadrons (protons, hyperons, deuterons) than for lighter ones (pions, kaons) if plotted against transverse kinetic energy $m_T - m_0$ or against p_T. This flattening of slopes is clearly seen in the BNL E802 data and somewhat less convincingly in the CERN experiments. While it has occasionally been interpreted in terms of different effective temperatures for different hadrons, it is more elegantly explained by our model hypothesis of collective transverse flow.

The model also makes predictions for differences in the spectral shapes for kaons and antikaons; however, these differences are small and hard to test without more accurate kaon data spanning a larger range of transverse momenta. One test is given by the different p_T-dependence of the K^+/π^+ and K^-/π^- ratios found by the E802 collaboration; we find good qualitative agreement with our model, while on a quantitative level the measured K^+ spectra appear to be even flatter than our prediction.

At CERN energies the pion spectra show a

pronounced enhancement at low $p_T < 200$ MeV/c. We find it very difficult to satisfactorily fit this effect with our hypothesis of transverse flow, in particular if realistic freeze-out surfaces are considered. While this disagreement affects only the region of very small transverse mass, $m_T < 400$ MeV, the discrepancy amounts to a large fraction of the total pion yield. Recent results from an analysis of resonance decay contributions to the pion spectrum indicate that ρ and ω meson decays after freeze-out may be responsible for this "anomalous" low-p_T shape [58].

The spherical model fails to reproduce the rapidity distributions measured at CERN, while the agreement with the lower energy Brookhaven data is reasonable [13]. This indicates that the idealization of a spherical fireball may be not too bad at AGS energies, where complete stopping of the projectile in the target has been observed, while it badly breaks down at CERN energies, where the collisions become partially transparent.

We argued that the presence of flow should show up in a definite p_T- and y-dependence of the slope parameters for the transverse mass spectra which can and should be further tested by experiment.

It has to be stressed that our description of the data uses the concept of a hot and thermalized *hadron resonance gas* for the fireball and at no point presupposes the formation of a quark–gluon plasma. On the other hand, the positive indications for flow give support to the idea that an extremely dense and quasi-equilibrated initial state has existed in these collisions, and this is an absolutely necessary condition for a possible phase transition to QGP during this stage. The initial energy densities extracted from our fits by back-extrapolating the amount of thermal and collective transverse flow energy to the initial state indicate rather large values, about an order of magnitude above the energy density in cold equilibrium nuclear matter and in the typical range where one would expect the beginning of a phase transition to QGP. As shown in several papers in [49], one obtains even larger energy densities by interpreting the measured rapidity densities via Bjorken's formula [14] in terms of a longitudinally expanding, boost-invariant firetube which was in thermal equilibrium already at a proper time of 1 fm/c. Also, if one describes the measured wide rapidity distributions in terms of a strong collective flow in the longitudinal direction which was created hydrodynamically (and is not due to the promordial longitudinal motion in a partially transparent collision) from an initial thermalized state with vanishing flow (Fermi–Landau model [15]), one again obtains [39, 40] much higher estimates for the initial energy densities. In all these cases one is led naturally to consider the possibility of QGP formation in the initial state. While it is, of course, still much too early to draw any conclusions in this respect, this road should clearly be further explored.

We would like to close with a few cautionary remarks: Since the concave curvature of the m_T-spectra is such an important ingredient in our transverse flow picture, and in the heavy-ion data it is clearly exhibited only in the pion spectra and in the deuteron spectra from E802, one has to worry about other possible origins for such a feature. Based on the experience from BEVALAC physics, resonance decays [17] come to mind, and an investigation of these in the context of ultrarelativistic nuclear collisions is under way. Also, even in pp spectra at these and higher energies a systematic flattening of the p_T-spectra at large p_T has been observed [6, 50]; it has been interpreted via the onset of hard QCD processes at large p_T (for a review see [17]). More along our line of thought, an interpretation in terms of an initial hot fireball has even been attempted for e^+e^- collisions [51], leading again to an effective temperature of ~ 200 MeV; to some extent a flattening of the spectra with increasing p_T can also be observed in this case [52].

Thus, it will be necessary to conceptually disentangle hard QCD processes from soft hydrodynamic effects before the flow interpretation can be considered fully convincing. The flow idea has been applied previously [53] to the charged particle spectra from cosmic ray events, although there a detailed test using different hadronic species was not possible. Also, similar features as discussed here, namely a flattening of spectra when going from pions through kaons to protons, which increased further when passing from peripheral (low multiplicity) to central (high multiplicity) collisions, were recently observed in the $p\bar{p}$ system at $\sqrt{s} = 1.8$ TeV [54]. This has also been interpreted [55] as evidence for fireball formation with collective transverse flow. Thus we seem to witness the resurgence, in a dynamical version which now includes collective flow aspects, of the 25 year old Hagedorn philosophy [56]. Its apparent success for even very small collision systems has not become less surprising by the years. Still more work has to be done to obtain a deeper understanding of all these old and new phenomenological successes.

Acknowledgements. We would like thank the WA80, NA34, NA35 and E802 collaborations (in particular R. Brockmann, C. Chasman, L. Dragon, H. Gutbrod, O. Hansen, B. Jacak, R. Renfordt, R. Santo, R. Stock, H. Ströbele, S. Wenig) for discussing with us the results from their experiments prior to publication.

References

1. K.S. Lee, U. Heinz: Z. Phys. C – Particles and Fields 43 (1989) 425
2. WA80 Coll. R. Albrecht et al.: GSI preprint GSI-89-03, submitted to Z. Phys. C; WA80 Coll. R. Santo et al.: Nucl. Phys. A498 (1989) 391c; L. Dragon: PhD thesis, University of Münster, 1989
3. NA 35 Coll. H. Ströbele et al.: Z. Phys. C – Particles and Fields 38 (1988) 89
4. NA 34 Coll. H.W. Bartels et al: Z. Phys. C – Particles and Fields 38 (1988) 85; NA34 Coll. J. Schukraft et al.: Nucl. Phys. A498 (1989) 79c
5. NA34 Coll. T. Åkesson et al: Z. Phys. C – Particles and Fields 46 (1990) 361
6. B. Alper et al.: Nucl. Phys. B100 (1975) 237; J.W. Cronin et al.: Phys. Rev. D11 (1975) 3105; D. Antreasyan et al.: Phys. Rev. D19 (1979) 764
7. NA35 Coll. A. Bamberger et al.: Z. Phys. C – Particles and Fields 43 (1989) 25
8. (a) NA35 Coll. J.W. Harris et al.: Nucl. Phys. A498, 133c (1989); (b) NA35 Coll. H. Ströbele et al., in: Hadronic matter in collision 1988, P. Carruthers, J. Rafelski (eds.) p. 357,

Singapore: World Scientific, 1989; (c) NA35 Coll. H. Ströbele et al., in: The nuclear equation of state, NATO ASI Series B, Vol. 216B, W. Greiner , H. Stöcker (eds.), p. 85. New York: Plenum 1990; (d) S. Wenig: PhD thesis, J.W. Goethe-Universität, Frankfurt, 1990
9. NA34 Coll. B. Jacak et al., in: The nuclear equation of state. NATO ASI Series B, Vol. 216B, W. Greiner, H. Stöcker (eds.), p. 125. New York: Plenum 1990
10. E802 Coll. P. Vincent, M. Sarabura, H. Hamagaki et al.: Nucl. Phys. A498 (1989) 67c, 409c, 415c; E802 Coll. S. Steadman et al., in: Hadronic matter in collision 1988, P. Carruthers, J. Rafelski (eds.), p. 607, Singapore: World Scientific 1989
11. E802 Coll. T. Abbott et al.: Phys. Rev. Lett. 64 (1990) 847
12. E. Schnedermann: Diploma Thesis, University of Regensburg, 1989; U. Heinz, K.S. Lee, E. Schnedermann, in: Quark–gluon plasma, World Scientific's Advanced Series on Directions in High Energy Physics, Vol. 6, R. Hwa (ed.), p. 471. Singapore: World Scientific 1990; U. Heinz, K.S. Lee, E. Schnedermann, in: The nuclear equation of state, NATO ASI Series B, Vol. 216B, W. Greiner, H. Stöcker (eds.), p. 388. New York: Plenum 1990
13. KLM Coll. H. von Gersdorff et al.: Phys. Rev. C39 (1989) 1385.
14. J.D. Bjorken: Phys. Rev. D27 (1983) 140
15. E. Fermi: Prog. Theor. Phys. 5 (1950) 570; L.D. Landau: Izv. Akad. Nauk. SSSR, Ser. Fiz. 17 (1953) 51; Collected papers of L.D. Landau, D. Ter Haar (ed.), p. 569. Oxford: Pergamon 1965
16. U. Heinz, K.S. Lee, M. Rhoades-Brown: Phys. Rev. Lett. 58 (1987) 2292; K.S. Lee, M. Rhoades-Brown, U. Heinz: Phys. Rev. C37 (1988) 1463
17. R. Hagedorn: Riv. Nuovo Cimento 6 (1983) 1
18. H.W. Barz, B. Kämpfer, B. Lukács, L.P. Csernai: Phys. Rev. C31 (1985) 268
19. H.W Barz, B.L. Friman, J. Knoll, H. Schulz: Nucl. Phys. A484 (1988) 661
20. P.R. Subramanian, H. Stöcker, W. Greiner: Phys. Lett. B173 (1986) 468
21. K.S. Lee, M. Rhoades-Brown, U. Heinz: Phys. Rev. C37 (1988) 1452
22. G. Bertsch, M. Gong, L. McLerran, P.V. Ruuskanen, E. Sarkkinen: Phys. Rev. D37 (1988) 1202; P.V. Ruuskanen E. Sarkkinen: private communication
23. F. Cooper, G. Frye, E. Schonberg: Phys. Rev. D11 (1975) 192
24. H. von Gersdorff, L. McLerran, M. Kataja, P.V. Ruuskanen: Phys. Rev. D34 (1986) 794; M. Kataja, P.V. Ruuskanen, L. McLerran, H. von Gersdorff: Phys. Rev. D34 (1986) 2755; J.-P. Blaizot, J.-Y. Ollitrault: Nucl. Phys. A458 (1986) 745
25. J.P. Bondorf, S.I.A. Garpmann, J. Zimányi: Nucl. Phys. A296 (1978) 320
26. In [1] constant local and global time hypersurfaces were inconsistently mixed in the evaluaton of the conservation laws and the spectra. We thank V. Ruuskanen for a clarifying discussion of this point
27. F. Cooper, G. Frye: Phys. Rev. D10 (1974) 186
28. P.V. Ruuskanen: Acta Phys. Pol. B18 (1986) 551
29. D. Kusnezov, G. Bertsch: Phys. Rev. C40 (1989) 2075
30. P.J. Siemens, J.O. Rasmussen: Phys. Rev. Lett. 42 (1979) 880
31. NA35 Coll. A. Bamberger et al.: Phys. Lett. B203 (1988) 320; NA35 Coll. M. Lahanas et al., in: The nuclear equation of state, NATO ASI Series B, Vol. 216B, W. Greiner, H. Stöcker (eds.), p. 145. New York: Plenum 1990
32. The small size of the deviations between Table 1a and 1b gives an indication of the unimportance of differences in the details of the freeze-out surfaces. The deviations from the numbers quoted in Ref. 1 are due to an error there, see [26], connected to the evaluation of the conservation laws. They affect mostly the initial temperature (and thus the specific entropy) and the kaon freeze-out point
33. P. Lévai, B. Lukács, J. Zimányi, U. Heinz: Z. Phys. A334 (1989) 77
34. P. Lévai, B. Lukács, J. Zimányi: J. Phys. G: Nucl. Part. Phys. 16 (1990) 1019; P. Koch C.B. Dover: Production of strange and nonstrange light nuclei in relativistic heavy-ion collisions, BNL preprint, 1989
35. C.M. Ko: Phys. Rev. C23 (1981) 2760
36. NA34 Coll. G. London et al.: HELIOS note 428, to appear in the proceedings of the International Europhysics Conference on High Energy Physics, Madrid, 1989
37. NA35 Coll. R. Renfordt et al.: Nucl. Phys. A498 (1989) 385c
38. R. Venugopalan, M. Prakash: Phys. Rev. C41 (1990) 221
39. J. Stachel, P. Braun-Munzinger: Phys. Lett. B216 (1989) 1; F.W. Pottag et al., in: Hadronic matter in collision 1988, P. Carruthers, J. Rafelski (eds.), p. 310. Singapore: World Scientific 1989
40. P. Braun-Munzinger, J. Stachel: Nucl. Phys. A498 (1989) 33c; J. Stachel, P. Braun-Munzinger: Nucl. Phys. A498 (1989) 577c
41. E802 Coll. T. Abbott et al.: Phys. Lett. B197 (1987) 285
42. E814 Coll. J. Barrette et al.: Phys. Rev. Lett. 64 (1990) 1219
43. U. Heinz, in: Hadronic matter in collision 1988, P. Carruthers, J. Rafelski (eds.), p. 517. Singapore: World Scientific 1989
44. S. Nagamiya, M. Gyulassy: Advances in nuclear physics, Vol. 13, p. 201; New York: Plenum, 1984. R. Stock: Phys. Rep. 135 (1986) 259
45. E802 Coll. Y. Miake, G.S. Stephans et al.: Z. Phys. C – Particles and Fields 38 (1988) 135
46. NA35 Coll. M. Gaździcki et al.: Nucl. Phys. A498 (1989) 375c; NA35 Coll. M. Gaździcki et al., in: The nuclear equation of state, W. Greiner H. Stöcker (eds.), NATO ASI Series B, Vol. 216B, p. 103, New York: Plenum Press 1990; NA35 Coll. J. Bartke et al.: Z. Phys. C – Particles and Fields in press
47. NA38 Coll. A. Baldisseri et al.: Annecy preprint LAPP-EXP-89-15, to appear in the Proceedings of the International Europhysics Conference on High Energy Physics, Madrid, 89; A. Baldisseri: Thesis, L.A.P.P. Annecy, 1990
48. P. Koch, U. Heinz, J. Pišút: Z. Phys. C – Particles and Fields 243 (1990) 149; 47 (1990) 477 Phys. Lett. B
49. Quark Matter '87, H. Satz, H.J. Specht, R. Stock: (eds.) Z. Phys. C – Particles and Fields 38 (1988)
50. UA1 Coll.: Phys. Lett. B118 (1982) 167
51. T.F. Hoang: Phys. Rev. D38 (1988) 2729
52. TPC/Two-Gamma Coll. H. Aihara et al.: Phys. Rev. D40 (1989) 2772
53. T.W. Atwater, P.S. Freier, J.I. Kapusta: Phys. Lett. B199 (1987) 30
54. E-735 Coll. C.S. Lindsey et al.: Nucl. Phys. A498 (1989) 181c; E-735 Coll. T. Alexopoulos et al.: Phys. Rev. Lett. 64 (1990) 991
55. L. Csernai, L. Gutay: private communication; E.F. Johansen et al.: University of Bergen Scientific Report 203/1989
56. R. Hagedorn: Nuovo Cimento Suppl. 3 (1965) 147; R. Hagedorn, J. Ranft: Nuovo Cimento Suppl. 6 (1968) 169; Y.P. Nikitin, I.L. Rozental: Theory of multiparticle production processes, Studies in High Energy Physics, Vol. 6, Harwood Academic Publishers 1988
57. E. Schnedermann, U. Heinz: manuscript in preparation
58. J. Sollfrank, P. Koch, U. Heinz: Regensburg preprint TPR-90-45, 1990, submitted to Phys. Lett. B.